Quantitative analysis of concentration gradient and ionic currents associated with hyphal tip growth in fungi

L. Limozin* and B. Denet
IRPHE–CNRS/Universités Aix-Marseille 1 et 2, Service 252, Faculté St. Jérôme, 13397 Marseille Cedex 20, France
(Received 17 December 1999; revised manuscript received 27 March 2000)

It has been shown previously that the nutrient gradient generated by a tip growing elongated cell induces an ionic current entering the cell tip and looping back in the extracellular medium [L. Limozin, B. Denet and P. Pelcé, Phys. Rev. Lett. **78**, 4881 (1997)]. We apply this mechanism to the case of hyphae of fungi, using realistic cell geometries, symport kinetics, proton pump permeabilities, and buffer concentrations. We show that this mechanism contributes to a noticeable part of the external current intensity, related inner electrical field and pH gradient, in agreement with experimental measurements. This provides a good example in biological cells of interaction between shape and field, a common property of growing nonliving systems, such as crystalline dendrites or electrodeposition.

PACS number(s): 87.17.Aa, 87.16.Uv

I. INTRODUCTION

Tip growth is the formation of tubes by fungal cells (hyphae), neurons (dendrites and axons), pollen grains or some algae (rhizoids). This growth mechanism involves the addition of new material at a very narrow area at the tip. The growth rate depends on the external medium and the tube orientation is very sensitive to external signals: among them, chemical (chemotropism) and electric (galvanotropism). These cells present a self-organization characterized by several tip to base gradients of diffusible substances (protons, calcium) and electrical potential in intra and extracellular media [1]. Experimental evidence indicates that these gradients are closely related to cell growth. Therefore, we can expect that they contribute to the self-organization of the system like a gradient of concentration or temperature in the case of a crystalline dendrite, a flame or in electrodeposition [2]. The interaction of shape and diffusion field in biological cells has been studied theoretically using analogy with physical systems [3]. In physical cases, a field keeps a uniform value along the interface, influencing the local velocity through the normal gradient. On a dual manner, for biological interfaces (the membrane separating extra and intracellular domain) a tangential gradient can be naturally created, with a possible physiological relevance. We provide here an example of such a self-organization in real cells, namely hyphae of fungi, in close relation with known biological literature.

The best quantitatively studied gradients are electrical fields which reflect a very common property of growing hyphae: an ionic currents circulation entering the tip, flowing across the cell, exiting farther from the trunk and looping back through the external medium [4]. *Neurospora Crassa* and *Achlya Bisexualis* have been extensively studied as models of growing fungal hyphae. These cells are tubes of 10–30 μm diameter and from 1 mm to many meters long. These rapidly growing tubes ($\sim$10 μm/min) and their exploring tip are particularly adapted to fungi way of life, they degrade and transform organic matter in media more or less rich in nutriments [5]. The intracellular potential is largely depolarized at the tip of *Neurospora Crassa* [6]. The pattern and order of magnitude of the external electrical potential was measured using a vibrating electrode [7]: this system allows one to measure local (on a 10 μm scale) potential differences with a sensitivity on the order of 1 nV. It appears that almost all hyphae generate an electrical potential loop, with positive charge entering at the tip and leaving the trunk 200 to 300 μm farther back ([8] in *Achlya Bisexualis*; [4] in *Neurospora*). On this length scale diffusion can be surely considered to dominate physiological convection [9]. The current intensity entering at the tip is between 0.1 and 1 μA/cm^2. Ion substitution experiments suggest that currents are carried by protons; this is confirmed by an external longitudinal pH gradient measured, basic at the tip and acid along the trunk. The proton-methionine cotransport system plays a crucial role in ionic circulation for *Achlya*, since removal of methionine almost abolishes the currents [8]. A similar role can be attributed to glucose for *Neurospora*. In many cases (but not all) abolition of currents stops the growth [4]. The internal electric field generated by this proton circulation is measured with intracellular microelectrodes and varies between 10 and 200 mV/cm, with the high value on the apical 400 μm [10].

In fungi, as in all plant cells, proton pumps maintain a negative cellular membrane potential by actively extruding protons in the external medium. Jennings [11] proposed three hypotheses to interpret tip depolarization [6] and ionic circulation:

(1) There are fewer pumps near the tip or equivalently more secondary transporters (by which protons enter the cell). This hypothesis of protein segregation is the most admitted by biologists and has been dicussed in terms of physical instabilities for symmetrical geometry [12]. However, it probably gives too small a size for current loops in the case of hyphae, as shown later in the paper.

*Present address: Phys. Dept., Technische Universität München, E22, James Franck Str., 85747 Garching, Germany. Email address: llimozin@ph.tum.de

(2) The membrane pump density is uniform, but their activity is reduced near the tip; this interesting hypothesis has been studied in *Neurospora* [13,14], assuming that the ATP which fuels the pump is reduced near the tip due to growing activity. We will come back to this interpretation at the end of this paper.

(3) The pump activity is uniform, but protons enter more by cotransport near the tip; we develop here this last possibility, showing that cotransport activity can be modulated along the shape by a concentration variation due to a geometrical effect, following [15].

The distribution of an absorbed nutrient diffusing around a tip-shaped cell is studied here with more generality than in this last paper. It is computed in direct analogy with a solute field around growing crystalline dendrites or metallic aggregates grown by electrodeposition.

In order to describe ionic circulation, we reduce the general system of reaction electrodiffusion equations involved in bioelectrical morphogenetic phenomena. Compared to the preliminary work [15], we add three major points, each having a crucial influence on current intensity predicted by our model: (i) the effect of the nonlinear flux of the symport, (ii) the role of geometry in a confined medium, (iii) the damping effect of pump current due to intracellular potential and pH variations.

The present study is divided in two parts: in the first part we describe the concentration of absorbed nutriment around a tip-growing cell without any coupling with electrical effects. A physical prototype with uniform solute flux through the membrane is first studied, showing the decrease of concentration from tip to base due to the elongated geometry. Then we take into account the weak nonlinear dependence on concentration which is characteristic of the symport flux. The concentration gradient induces a flux variation along the shape, but is damped by dissipation through the symport. We evaluate the effect of the proximity of growing cells in an hyphal colony: the confinement increases greatly the gradient obtained in a medium of infinite extension. We conclude this part by discussing the possible feedback effect of the gradient on growth using quantitative results of chemotropism experiments in *Achlya*. In a second part, we add the electrical effects and we are interested in calculating the potential and pH gradient created by a circulation of protons both in external and internal media. Using reduced reaction electrodiffusion equations, we can compute analytically these quantities for unidimensional diffusion in the cell. The currents of both a symport segregation or a differential symport activity due to the previous external amino-acid gradient are then calculated and compared. We, finally, compare our mechanism with the other interpretations of current generation available in the literature.

II. EXTERNAL ''NATURAL'' CONCENTRATION GRADIENT

We study the concentration distribution in the external medium of a neutral nutrient absorbed by a tubular cell of radius R and length $2l \gg R$ with a flux J through the membrane. We assume that the typical time of the problem is given by the advection time due to tip growth, and is therefore slow compared to diffusive processes [9]. Therefore, the solute is diffusing with the coefficient D in the quasistationary regime and its concentration is the solution of a Laplace equation. In Secs. II A and II B, the medium is of infinite extension, and the reference concentration c_∞ is given far from the cell. In this way we free ourselves from external length scales. In Sec. II C the medium is confined, and the boundary conditions will be precise there. We note as s the curvilinear abscissa measured along the cell, starting from the tip. We are interested in the concentration in the vicinity of the membrane along the cell.

The cell shape is defined by an hyphoid curve [16] for which the equation in cylindrical coordinates is $z = \rho \cot(\pi\rho/R)$ where R is the radius at the base. We cut this tip-rounded tube at the length l and impose the symmetric boundary condition at this base. To compute c we use a singularity method which is inspired from two-dimensional (2D) simulation of crystal dendritic growth [17]. For a 3D axisymetric problem in an infinite extension medium, we only calculate both c and its normal derivative $\partial c/\partial n$ along a generating line of the shape. Corresponding equations are given in Appendix A. In a confined medium (hyphae in a colony, Sec. II C), we have also used in parallel a finite element software FREEFEM developed by Pironneau and Prud'homme (freeware available at www.asci.fr). In this case, we have in general obtained similar results with both methods.

A. Uniform flux: Geometrical effect

For simplicity of the analysis, we assume here that the membrane flux $J>0$ (along the normal to the cell surface, entering in the cell) characterizing the nutrient absorption is uniform. Qualitatively, we expect that concentration would decrease along the tube from tip to base because the absorbing surface is smaller at the tip (seen like a sphere of radius R) than at the base (seen like a cylinder of radius R). From dimensional considerations, the nutrient concentration can be written

$$c(s) = c_\infty \left[1 - \frac{JR}{Dc_\infty} f(s) \right],$$

where f only depends on s/l and R/l. In Fig. 1 we show numerical curves of concentration along the tube as a function of distance from tip, for two different radius R. We use an analytical approximation at distance $s \geqslant R$ from the tip:

$$f(s) \simeq 1 + \frac{1}{2} \ln\left(\frac{ls}{R^2} \right). \tag{2.1}$$

At the base (or center) of the cell ($s=l$), this formula can be interpreted like this: sufficiently far from it, the cell can be seen like a monopole which produces the same concentration field as a sphere of equal surface, i.e., of radius $\sqrt{Rl}$: $c(r) = c_\infty - (Jl/D)(R/r)$ where r is the distance from the center. Assuming that this field is not very disturbed at the tip, the concentration is ($r \sim l$): $c_t \simeq c_\infty(1 - JR/Dc_\infty)$ and we assume that this concentration line is almost spherical. At the base ($r \sim R$), the field c_b is the one produced by a long cylinder; then between $r=R$ and $r=l$, we get $c_t - c_b$

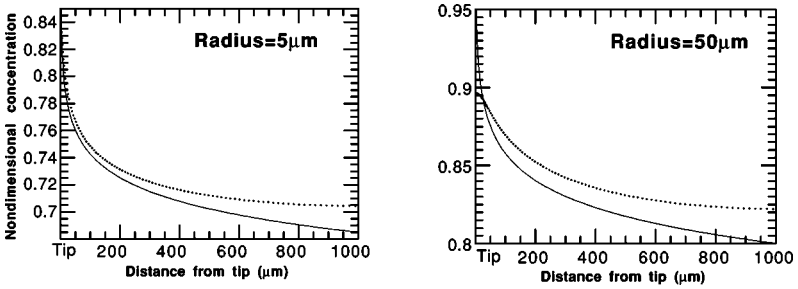

FIG. 1. Nondimensional concentration profile c/c_∞ along a hypha of radius $R=5\ \mu$m or $R=50\ \mu$m and length $l=1$ mm. Dashed line is numerical calculation and solid line is calculated with Eq. (2.1).

$=(JR/D)\ln(l/R)$ and deduce the value of $f(l)=1+\ln(l/R)$ which coincides with Eq. (2.1).

This formula does not describe concentration profile near the tip, where the gradient should vanish by symmetry. Figure 2 is a magnification of Fig. 1 at the vicinity of the tip, showing the amplitude of the natural gradient which can feedback on growth (see Sec. II D).

In a limited but isotropic external medium, we can suppose that a concentration c_0 is given at a distance r_{max} from the base of the tube. In this case, the previous results are the same if taking $c_\infty=c_0+(JR/D)(l/r_{max})$; we numerically checked this as long as $r_{max}-l\gg R$.

$X=JR/DC_\infty$ scales the concentration difference between the cellular membrane and far from the cell. When $X\gg 1$, concentration near the cell is given by JR/D; when $X\ll 1$ this concentration is almost c_∞. This parameter is useful to study the influence of an external signal on the cell.

$(JR/D)\ln(l/R)$ gives the concentration difference between tip and base; its magnitude determines the current loop intensity described in the second part of this paper.

Relative variation of concentration between tip and base has to be evaluated to examine a possible feedback effect of the gradient on growth. In particular, we evaluate relative concentration differences in the tip area (Sec. II D).

B. Michaëlis-Menten flux: Gradient damping

Generally, the entering membrane flux J depends on local external concentration and can be described by the classical Michaëlis-Menten kinetics: $J(c)=J_m[c/(c+K_M)]$ where J_m is the maximal flux of the transporter and K_M its affinity to the substrate, taken here as a variable parameter. This kinetics is appropriate to describe the flux of a nutrient absorbed by symport with protons, assuming that the transporter is saturated by protons [18]. For high affinity ($K_M\ll c$), the flux is saturating at J_m; for low affinity ($K_M\gg c$), flux and concentration are proportional (the equivalent of a radiating boundary condition in thermal sciences). For mass diffusion, we define the number $N=J_mR/DK_M$ by analogy with the Nusselt number which characterizes heat transfer between a solid body and its environment. Around a spherical cell, concentration near the membrane reads $c_m=c_\infty/N+1$. When $N\ll 1$, $c_m\simeq c_\infty$: resistance to solute transport principally occurs in the membrane; when $N\gg 1$, $c_m\ll c_\infty$, and resistance to the solute transport occurs in the solution.

In the high affinity limit ($K_M\ll c$), we return to the previous case of uniform flux: the concentration difference between tip and base is maximal and is due to the geometrical effect. However, the variation of flux due to concentration is small. For lower affinities, dependence of flux on concentration is large; but dissipation occuring in the membrane reduces both the flux and the concentration gradient due to the geometrical effect (Fig. 3, left).

Therefore, we expect that the flux difference between tip and base reaches a maximum for intermediary values of the affinity. This is shown on Fig. 3 (right), where this difference $J_{tip}-J_{base}/J_m$ is drawn as a function of K_M and shows a maximum at $K_M^*=0.02$ mM. Affinity measurements give a large range of values (between 1 μM and 1 mM) depending on species and transport system type. Nevertheless, $K_M=10\ \mu M$ is a typical value for methionine transport [19,20]. The parameters are chosen to describe the absorption of methionine ($c_\infty=0.1$ mM, $D=5\times10^{-10}$ m^2/s) by a hypha of *Achlya Bisexualis* ($R=15\ \mu$m and $l=1$ mm) through a methionine/proton symport ($J_m\simeq 5\times10^{-7}$mol/m^{2}s and K_M between 1 μM and 1 mM [8,10,20]).

C. Confined medium: Gradient magnification

In a more realistic view, hyphae can be considered to be grown in a colony. In a first configuration, hyphae are growing by creeping along a gel substrate. The nutrient concentration is fixed by a continuous flow in which the other face of the gel of thickness L is soaking. For a dense mycelium, the culture can be taken as planar; we consider a slide of mycelium with length l and thickness $2R$. Concentration c_∞ is given at the distance L (Fig. 4, 2D). This geometry was examined previously for simplicity [15]: when symport is in

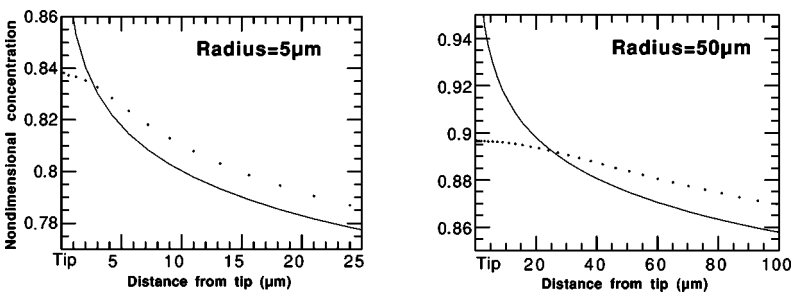

FIG. 2. Same profiles as Fig. 1 in the tip area.

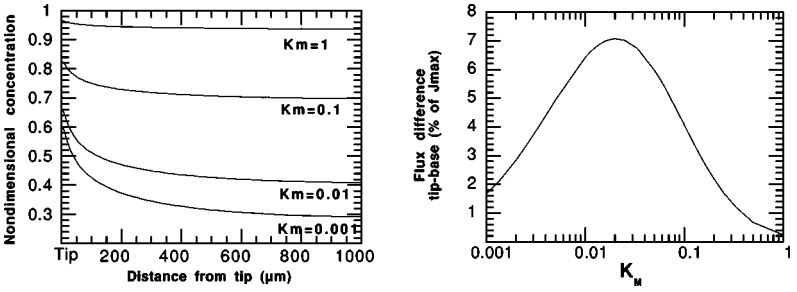

FIG. 3. Left: Effect of symport affinity K_M (mM) on variation of nondimensional concentration c/c_∞ along a hypha. Parameters (SI): $J_{max}=5\times10^{-7}$, $D=5\times10^{-10}$, $c_\infty=0.1$. Hyphal radius $R=15$ μm. Right: Flux difference between tip and hyphal base divided by J_{max}, as a function of affinity K_M (mM).

the linear regime ($K_M=1$ mM), the concentration gradient reaches 30% along a $l=1$ mm cell (Fig. 5 left).

More frequently hyphae are growing off from the gellose substrate into the tridimensional aqueous medium. This experimental configuration allows measurements with the vibrating probe. We note L_1 as the average distance between individual hyphae, and L_2 is the distance of the substrate at which the nutrient concentration is assumed to be uniform at c_∞. Each hypha is then assumed to be contained in a cylinder of diameter L_1 with zero flux boundaries conditions, except at the top section (at distance L_2 from the base of the hypha), where c is fixed at c_∞ (Fig. 4, 3D). We emphasize that this geometry is the same, at a smaller scale, for microvilli of intestinal epithelial cells or some sensorial cells. We can expect analogous physical self-organization in these systems. When $L_1 \ll l$, diffusion is almost unidimensional in the axial direction and nutrient concentration can be calculated either:

In the linear limit of the symport ($K_M \gg c$), we get the profile along the hypha:

$$c(z)=c_\infty \frac{\cosh z/\delta}{\cosh l/\delta+\dfrac{L_2-l}{\delta}\sinh l/\delta} \tag{2.2}$$

with characteristic length $\delta=L_1/2\sqrt{DK_M/2J_{max}R}$ (dotted line in Fig. 5 right), or

In the saturated limit, the profile is parabolic:

$$c(z)=c_\infty\left\{1-\frac{J_{max}R}{Dc_\infty}\left(\frac{2l}{L_1}\right)^2[2L_2/l-1-(z/l)^2]\right\}.$$

When $K_M=K_M^*$, which maximizes the flux variation in the nonconfined medium, symports at the tip are saturated; but concentration decreases rapidly along the hypha and the base is in a linear regime. The numerically computed flux profile is well fitted by an exponential curve. For example, when $L_1=400$ μm, the flux decreases almost 60% from tip to base on a characteristic length $l_s=350$ μm.

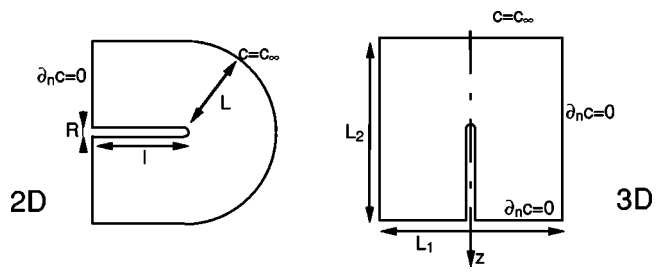

FIG. 4. Geometry and boundary conditions for two-dimensionnal culture on a substrate (2D) and in a tridimensional solution (3D), where a colony of periodically distributed hyphae (distant of L_1) are growing vertically (direction -z).

D. Possible feedback on growth and conclusion

We compare the intensity of the natural gradient produced by the tip shape and the ones externally imposed to reorient the growth. In such experiments of chemotropism [21], a pipette containing one amino-acid is placed 100 μm above the hypha and is shifted away the same distance from the axis. The tip growth can be reoriented in the direction of the pipette containing methionine as soon as the concentration difference felt across the tip exceeds 1%.

Now for a hypha of radius 15 μm with saturated symport in an infinite medium, calculated methionine concentration steps from 0.615 c_∞ to 0.595 c_∞ on the first 15 μm at the tip (see also Fig. 2). Theoretically, this natural gradient of 3% is sufficient to influence or even sustain tip growth. According to Schreurs [21], the chemotropic effect could be mediated by specific methionine receptors: when they are not saturated, they can feel a great natural gradient produced by saturated symports. Moreover, the maximum of variation is localized at the tip growing region, a very restricted area of 20 μm near the apex [22].

As a conclusion for this part, we have shown that hyphal cells create a natural concentration gradient of absorbed nutrient along their shape. In close analogy with the crystalline dendrite, this gradient is strong enough to feedback on growth, if the nutrient has morphogenetic properties. In the next part, we will show that the differential activity of the symport between tip and base is sufficient to be at the origin of the ionic circulation measured in these cells.

III. IONIC CURRENTS

A. Reduction of reaction-electrodiffusion equations

Ions circulating in biological cells are put in motion by active transport (energy is provided chemically by ATP) through the membrane and diffuse in external or internal medium. In solution, their motion obeys Nernst-Planck electrodiffusion equations with chemical reaction terms. The system is closed with the Gauss equation linking the electrical field divergence with the charge density. Larter and Ortoleva presented a multiscale approach to reduce these equations and applied it to self-electrophoresis [23]. With similar assumptions, we educe this system as follows.

The characteristic time scale of morphogenetic processes exceeds 1000 s. Therefore, we can neglect the capacitive effects of the membrane (1 ms) which are caused by the localized space charge contained in the Debye layer. As

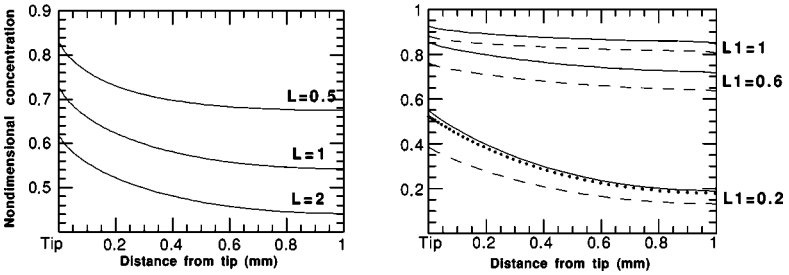

FIG. 5. Left: 2D medium, concentration profiles for varying mycelial thickness L (mm). Right: 3D confined medium, concentration profiles at $K_M=1$ mM for varying interhyphal distance L_1 when reference concentration is fixed at L_2 (plain curve $L_2=2$mm; dashed curve $L_2=1.5$ mm; dot line is formula 2.2 for $L_1=0.2$ mm and $L_2=1.5$ mm).

shown in [24], it is not possible to obtain fast electrical instabilities with this assumption. However, we can get in this way the slow diffusive instability proposed by Léonetti and Dubois-Violette [25] as proven in [26].

The characteristic length scale is the cell's diameter (minimum 10 μm). First, we neglect the Debye layer surrounding the membrane where space charge is nonzero: for typical ionic strength, its thickness is of the order of a few nm. Second, we suppose that chemical reactions are fast: a typical time scale for an acido-basic reaction is $\tau_R \sim 10^{-6}$s. If protons are crossing the membrane, their reaction with some buffer will occur in a thin reactive layer of negligible thickness $\lambda_R \sim \sqrt{D\tau_R} < 0.1$ μm [26].

Outside of these layers, the electroneutrality condition is fulfilled and reactions are equilibrated. The system can be written in terms of effective diffusion equations for each species. As explained above, for slow processes like growth, a quasistationarity assumption leads to Laplacian equations, which are verified by each species concentrations and by potential.

B. Effective boundary conditions and physical properties

In Appendix B, we combine Nernst-Planck flux $\vec{J} = -D(\vec{\nabla}c + zc\vec{\nabla}\psi)$ to derive effective boundary conditions for quasistationary diffusion of reacting charged species crossing a membrane. As mentioned in Appendix B, the correct quantitative description of protons and potential requires the introduction of major biochemical ingredients, namely buffers and counterions (see Table I). Buffers are either mobile (notation M, diffusion coefficient $D \neq 0$, typically phosphates or carbonates), or fixed (notation $F, D=0$). These latter buffering sites are located in both some lipids of the membrane (plasmic and from internal organelles) and in some amino-acid constituting proteins, for example from the cytoskeleton. They are consequently bound to some cellular structure and are therefore not diffusing. We relate real fluxes at the membrane to the gradient in the bulk of solution, by writing a conservation of chemical species through the Debye and reactive layers.

Real fluxes J^m through membrane proteins depend, in principle, on local concentration and potential, i.e., inside the double layers. We suppose that we can replace these local values by values outside of the layers, and that effective permeabilities compensate for a possible difference between these values.

We note that a passive ion (not actively transported at the membrane), which does not react with protons, is at rest in a stationary regime. It can be understood by remarking that, first, the flux divergence vanishes (conservation of the species in the stationary regime, without chemical reaction). Second, if the flux through the membrane is passive, it can be written everywhere as a gradient and its rotational is therefore zero either in external, internal media and through the membrane. These two conditions force the flux to vanish. This extends Ferrier's results [27] where nontransported species at the membrane remain at equilibrium in the entire medium.

Generally, charged forms of buffers cannot cross the membrane in the absence of specific transporters. Physiological buffers with a neutral form able to directly cross the membrane have generally a $pK \ll pH$ (which implies $\alpha \simeq 1$, with the notation of Appendix B); we therefore neglect the leak of protons due to membrane permeability to the mobile buffer: $J_M^m = J_{HM}^m = 0$.

Moreover, when the flux of the counterion can be neglected ($J_K^m = 0$), variations of pH and potential are directly proportional, according to

$$\frac{\delta pH}{\delta \psi} = \frac{\Sigma z_k^2 c_k}{[H](\gamma_F + \gamma_M)}, \tag{3.1}$$

which comes from the third equation of system (B1) of Appendix B and where we noted

$$\gamma_F = \frac{c_F K_F}{([H]+K_F)^2}, \quad \gamma_M = \frac{c_M K_M}{([H]+K_M)^2}.$$

TABLE I. Parameters values. Proton H, mobile buffer M, fixed buffer F, potassium K, dimensionless electric potential ψ.

Species	H^+	M+HM	F_1/F_2	K^+	ψ
External (mM)	$pH_e=6.5$	$c_{Me}=1$		1	0
Cytoplasm (mM)	$pH_i=6.9$	$c_{Mi}=2$	150/100	200	-5.2
Equil. const.		$pK_M=6$	6/8.5		
Permeability (m/s)	10^{-3}–10^{-2}	5×10^{-5}		5×10^{-7}	
Diffusion (m^2/s)	10^{-8}	10^{-9}	0/0	2×10^{-9}	

At the numerator is the ionic force which damps potential variations. At the denominator, the buffering power, which damps pH variations. Furthermore, we can express potential variations as a function of membrane proton flux in a spherical cell of radius R:

$$\delta\psi = -\frac{RJ_H^m}{D_{Heff}[K^+]}$$

with the effective diffusion coefficient $D_{eff}=(D_H+\gamma_M D_M)/(1+\gamma_M+\gamma_F)$. We get here an expression first derived in more restrictive conditions [28]. Hence the potential gradient is increased by the presence of fixed buffers, which create a gradient of fixed charged and an associated electrostatic potential. This effect is reduced by the presence of mobile buffers which concurrently bind and carry protons. We emphasize here that the effective conductivity which appears in the tension-current relation can differ very much from its classical measurement in electrolyte, using an externally imposed voltage gradient. This is due to the fact that in bioelectric phenomena, the electrical field is not imposed by an external source but is only a consequence of ionic differential diffusion. Consequently species are not carrying current proportionally to their concentration, but depending on the way they are actively transported at the membrane.

C. Membrane flux for symports and pumps

We assume that the current loop on hypha is generated either by the nonuniformity of the symports distribution (segregation), or by the nonuniformity of symports activity, due to the external gradient. In both cases, we can write the variation of proton influx through the symports on the characteristic length l_s as $\delta J_s \sim \delta J[e^{-z/l_s}-l_s/l]$, the function of the longitudinal coordinate z.

We take for the proton pump flux:

$$J_p = a\frac{K_p^*[H]_i}{K_p+[H]_i}(\psi_m-\psi_p) = \frac{J_p^{max}[H]_i}{K_p+[H]_i}$$

with a saturating constant for protons K_p between 10^{-5} and 10^{-4} mM; a reversal potential for current $\psi_p=-13$; a maximal flux $J_p^{max}=aK_p^*(\psi_m-\psi_p)$ with aK_p^* between 10^{-7} and 10^{-6} mol/m^{2}s. Parameters are chosen to fit the current-voltage characteristic of the pump obtained by Sanders [29]. Hence pump permeability to protons is

$$P_H = \frac{\partial J_p}{\partial[H]_i} = \frac{J_p^{max}K_p}{(K_p+[H]_i)^2} \simeq 10^{-3}-2\times10^{-2} \text{ m/s},$$

with cytoplasmic pH around 7. The perturbation on symport proton current is damped by the dependance of pump current in both potential and pH. This damping is represented by the total permeability of the pump:

$$P = \frac{\overline{J_p}}{[H]_i}\left(\frac{K_p}{K_p+[H]_i}+\frac{1}{\overline{\psi_m}-\psi_p}\frac{[H]_i}{K_F+[H]_i}\right) = P_H+P_\psi,$$

where we introduced relation (3.1). When $pK_F=6$ [30], P is approximately between 10^{-3} and 10^{-2} m/s. We note $\lambda_c=\sqrt{DR/2P}$ as the damping length where there appears the real cytoplasmic diffusion coefficient of protons

$$D = \gamma_M D_M\left(1+\frac{[H]}{[H]+K_F}\right) \simeq 2\times10^{-6} \text{ m}^2/\text{s}.$$

Parameters values are summarized in Table I and are taken from [8,14,30].

D. Elongated cell: unidimensional internal diffusion

We consider the loop of a diffusing species circulating inside and outside of a tubular cell of radius R. If $\lambda=1/k$ is the size of the loop, the ratio of internal to external concentration multiplied by diffusion coefficients is

$$\frac{D_i c_i}{D_e c_e}(R) = -\frac{K_1 I_0}{I_1 K_0}(kR),$$

where I and K are the modified Bessel functions. This ratio scales as $2/[\ln(kR)(kR)^2]\sim100$ when $kR\sim0.1$. Because current loop size exceeds ten times the cell diameter, external species variations are negligible compared to internal ones. In particular, variations of membrane potential $\psi_m=\psi_i-\psi_e$ are entirely due to internal potential.

A second geometrical simplification consists in assuming an unidimensional diffusion inside the cell, along the axis. This is again true when $\lambda \gg R$, where λ scales as the size of the phenomenon.

Under the different previous assumptions, the proton concentration inside the cell satisfies the following equation:

$$\lambda^2\frac{d^2h}{dz^2}-h = J_s/P,$$

which is analogous to the stationary cable equation used in classical electrophysiology. We compute both h and the total proton flux J as functions of distance from tip:

$$h(z) = \frac{\delta J/P}{x^2-1}(x^2e^{-z/l_s}-xe^{-z/\lambda_c})-\delta J/P\frac{l_s}{l},$$
$$J(z) = \frac{\delta J}{x^2-1}(e^{-z/l_s}-xe^{-z/\lambda_c}). \tag{3.2}$$

We note $x=l_s/\lambda_c$ as the ratio of flux perturbation length l_s to the damping length λ_c. The entering flux at the tip reads $J(0)=-\delta J/(1+x)$, the distance where currents reverse (or current loop size): $z_0=l_s[\ln x/(x-1)]\sim l_s$, the maximum exiting current:

$$\delta J\frac{x^{\frac{1+x}{1-x}}}{1+x}.$$

E. Membrane protein segregation

The usual explanation for current loops in *Achlya* involves an increase of symport density at the tip [8,31] (or a decrease of pumps density). Even if this hypothesis is the simplest, proposed mechanisms to support protein segrega-

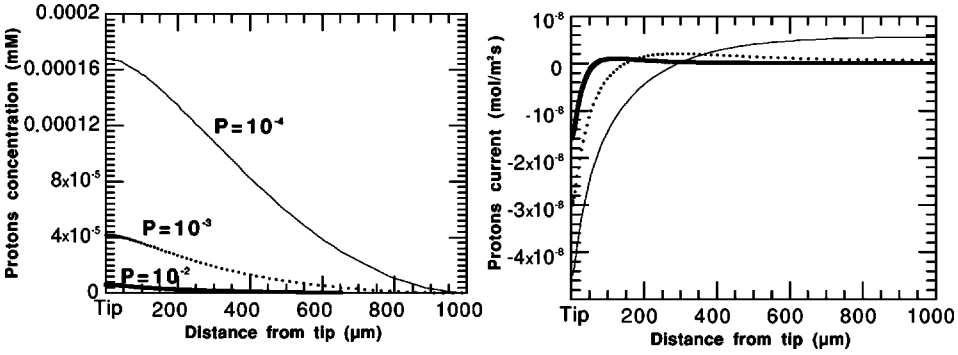

FIG. 6. Longitudinal distribution of free protons in a hypha (relative to a mean value) and of currents caused by the external methionine gradient in illimited medium.

tion and observations are rare. We can then argue that this segregation is possible through the binding of symports to specific cortical cytoskeletal structure (for example stretch-activated receptors for calcium [32]). This prevents proteins from being advected by the front-rear membrane flow due to growth, in the frame of the tip. In this hypothesis, the length l_s should be around 10 μm, the size of actin cortex. By this mechanism, the current loops size, of the order of l_s, remains largely shorter than observations.

The second possibility is that membrane proteins are kept at the tip by electrophoretic or electro-osmotic forces. Electrophoresis is too weak to move proteins at tip growth rate (~ 10 μm/min) even with the strong internal measured electric field [15]. A cytoplasmic streaming (possibly of electroosmotic origin) is observed, reaching speed greater than the tip growth rate. In this case proteins in the membrane could be distributed with large scale gradient and then generate large scale currents loops. However, a segregation mechanism involving slow movements of proteins in the membrane cannot explain a rapid response of current to medium change.

F. Differential symport activity due to the natural gradient

We examine now the effect of the differential activity of symports along the cell due to the external methionine gradient. In the medium of infinite extension, gradients of protons and currents are given in Fig. 6 for different total permeabilities P of the pump. Currents are of weak magnitude, and pH gradients are strong for low permeability.

In a colony the large methionine gradient is defined with $\delta J \sim J_{max}/2$ and $l_s \sim 300$ μm (affinity $K_M = 0.01$ mM and maximal flux $J_m = 10$ μA/cm^2, interhyphal distance $L_1 \sim 500$ μm). For two values of the total pump permeability P, different characteristics of the proton loop are summarized in Table II.

Experimental measurements are well fitted for a permeability $P = 10^{-3}$ m/s. Taking into account these results, it is clear that ionic currents in *Achlya* can largely be caused by the external methionine gradient.

IV. DISCUSSION

In this paper we have addressed the question of whether diffusion gradients naturally produced by elongated cells could account for physiological phenomena. This problem is attractive because of its analogy with physical growth phenomena. Taking the example of fungal hyphae in realistic conditions, the answer is positive as far as ionic currents are manifestations of cellular physiology. This is a striking example of the interaction of shape and field in the living world, a phenomenon usual in nonliving growth. However, due to the complexity of the system, we mention some points which will require a deeper analysis.

The quantitative estimation of currents is principally based on symport characteristics: maximal flux J_m and affinity K_M. However, these parameters have been scarcely measured and we have extracted values indirectly from the literature. Moreover different symport types with different affinities can be found with the same substrate. Parameters for methionine cotransport should, therefore, be carefully measured in *Achlya*. The natural concentration gradient we evaluate for methionine should occur for every absorbed nutrient. Every amino acid and nutrient like sugar is cotransported in plant or fungal cell with protons. There are additionnal contributions to proton currents from all these symports, each depending on a parameter J_m and K_M. These effects can greatly increase our estimation of currents due to natural gradients.

This model predicts a large cytoplasmic pH gradient (see Table II), acidic at the tip. Contradictory measurements are given in the literature: basic pH at the tip [33] in *Neurospora* or no detectable gradient in *Saprolegna* [34] or *Neurospora* [35]. It is argued that the use of intracellular probes could disturb the real gradient and distort measurements. Nevertheless our modeling of intracellular pH is extremely simple. We neglect acids produced by metabolism, which are an internal source of protons exiting from mitochondria. Relation (3.1) fitting the ratio of pH and potential variation, is still valid in this case because it does not depend directly on the presence of internal sources. But this relation imposes $\delta pH > \delta\psi$ which is not consistent with both electrical and pH

TABLE II. Characteristics of the proton current loop generated by the methionine gradient in a confined medium, as a function of the total pump permeability P.

Permeability P	m/s	10^{-2}	10^{-3}
Tip current	μA/cm^2	-0.5	-1
Base current	μA/cm^2	0.05	0.2
Currents inversion	μm	100	200
$\delta[H]_i$ sur 1 mm	mM	5×10^{-5}	4×10^{-4}
δpH_i sur 1 mm		0.2	0.6
$\delta\psi_i$ sur 1 mm($K_F \gg [H]_i$)	RT/F	0.05	0.4
$\delta\psi_i$ sur 1 mm($K_F \sim [H]_i$)	RT/F	0.2	1
δV_m sur 1 mm($K_F \sim [H]_i$)	mV	5	25

gradient measurement. However, for charge conservation, an internal source of proton should be compensated by expulsion of cations through the membrane, for instance, potassium. In this case the potassium flux is not negligible, which invalidates Eq. (3.1): this effect could, therefore, give a relation between pH and the potential which matches with experiments.

We showed that in the case of *Achlya*, segregation of transport proteins could hardly be extended enough to explain large current loops. However, segregation is not incompatible with our mechanism of differential activity. It seems clear that in some systems like pollen tube or certain fungi, currents are primarily caused by a spatial separation between pumps which expels protons and symports which bring protons into the cell. By its simplicity, the mechanism described in this paper is very generic for all tip-shaped cells but only explains currents entering at the tip. Segregation could relay it to account for exiting apical currents in old hyphae of *Achlya* [36].

The present mechanism links current circulation with elongated shape, and indirectly with growing tubes: first, because shape is a consequence of growth process; second, because gradients of nutrients and thus currents are a proof of cell health (and growth, in the case of hyphae). In a previously described mechanism [13], growth and current are related more directly. Apical endothermic growing activity is expected to be responsible for a cytoplasmic ATP deficit in the tip region. Consequently, pumps close to the tip are less fueled with ATP and their proton expelling activity is reduced: protons enter preferentially at the tip. Conversely, pumps far from the tip expel more protons to maintain membrane potential in the entire cell. Currents can be seen as an energy transfer from base to tip in order to keep tip membrane potential sufficently polarized. This interesting hypothesis should be carefully examined, taking into account very complex cytoplasmic ATP regulation. An internal ATP gradient has already been predicted in intact epithelial renal cells [37]. As with calcium for signaling, a study of such an ATP gradient would be of great importance to explore cell energetics. We notice that the theoretical framework for such a future study is already provided in this paper, since protons and ATP are both produced in mitochondries, consumed by pumps at the membrane and are probably effectively diffusing in the medium.

ACKNOWLEDGMENT

The authors would like to especially thank Pierre Pelcé for numerous and useful discussions.

APPENDIX A: NUMERICAL METHOD

The problem is to solve a Laplace equation $\Delta\phi=0$ inside and outside of a closed continuous surface Σ of space. We define the Green function of the Laplace equation in 3D for two points of space M and P (P is usually describing the surface): $G(M,P)=-1/4\pi MP$. The integral equation relating G and ϕ reads

$$\forall M\in\Sigma,\ \int_\Sigma \phi(P)\frac{\partial G}{\partial n_P}(M,P)d\Sigma_P+\frac{\alpha(M)}{2\pi}\phi(M)=\int_\Sigma \frac{\partial\phi}{\partial n_P}G(M,P)d\Sigma_P, \tag{A1}$$

where $\alpha(M)$ is the angle of Σ in M ($-\pi$ in the interior, π in the exterior, $\pm\pi/2$ in a corner with right angle). Because of axisymmetry, we can integrate G according to the angular coordinate θ (we note ρ, z as the two other cylindrical coordinates)

$$G^*(\rho,z|\rho',z')\equiv\int_0^{2\pi}G(\vec{r},\vec{r}')\rho'd\theta'=-\frac{\rho'}{\pi\sqrt{D}}K\left(\sqrt{\frac{4\rho\rho'}{D}}\right)$$

with $D=(\rho-\rho')^2+(z-z')^2+4\rho\rho'$ and $K(k)=\int_0^{\pi/2}[d\theta/(1-k^2\sin^2\theta)]$ (elliptic function of the first kind). We define also

$$\begin{aligned}H^*(\rho,z|\rho',z')&\equiv\int_0^{2\pi}\vec{\nabla}_{\vec{r}'}G(\vec{r},\vec{r}')\cdot\vec{n}(\vec{r}')\rho'd\theta'\\&=-\frac{1}{2\pi D^{3/2}}\{-Dn_{\rho'}K(k)\\&\quad+[(\rho^2-\rho'^2+(z-z')^2)n_{\rho'}\\&\quad+2\rho' n_{z'}(z-z')]\Pi(k^2,\pi/2,k)\}\end{aligned} \tag{A2}$$

with

$$\Pi(k^2,\pi/2,k)=\int_0^{\pi/2}\frac{d\theta}{(1-k^2\sin^2\theta)^{3/2}}$$

(elliptic function of the second kind). Following [17], we discretize Eq. (A1):

$$\sum_j G_{ij}q_j=\sum_j H_{ij}u_j,$$

where u is the field and $q=\partial u/\partial n$ is its normal derivative along Σ. H includes $[\alpha(M)/2\pi]\phi(M)$ and H_{ii} is calculated by $H_{ii}=-\Sigma_{j\neq i}H_{ij}-1$. Influence coefficients are integrals calculated by a Gauss quadrature. G_{ii-1},G_{ii},G_{ii+1}, H_{ii-1},H_{ii+1} diverge logarithmically and are treated separately.

APPENDIX B: BOUNDARY CONDITIONS

Protons H are diffusing with coefficient D_H in a medium containing mobile buffers M (charge z_M, diffusion D_M), fixed buffers (charge z_F), and counterions (z_K,D_K). We establish here the relations between membrane flux (with m superscript) and gradients in the bulk. In the quasistationary regime, the total flux of chemical species H, M, and K are conserved between membrane and bulk, i.e., through the reactive layer and the Debye layer:

$$\vec{J}_M^m+\vec{J}_{HM}^m=\vec{J}_M^{tot}=-D_M\{\nabla[HM]+(z_M+1)[HM]\nabla\psi + \nabla[M]+z_M[M]\nabla\psi\},$$

$$\vec{J}_H^m+\vec{J}_{HM}^m=\vec{J}_H^{tot}=-D_H(\nabla[H]+[H]\nabla\psi) - D_M\{\nabla[HM]+(z_M+1)[HM]\nabla\psi\},$$

$$\vec{J}_K^m=\vec{J}_K^{tot}=-D_K(\nabla[K]+[K]\nabla\psi)$$

with dimensionless electrical potential $\psi=e\phi/RT$. In the bulk, chemical reactions are equilibrated and electroneutrality is fulfilled:

$$HM\rightleftharpoons M+H \quad K_M=\frac{[H][M]}{[HM]}, \quad c_M=[HM]+[M],$$

$$HF\rightleftharpoons F+H \quad K_F=\frac{[H][F]}{[HF]}, \quad c_F=[HF]+[F],$$

$$[H]+z_F[F]+(z_F+1)[HF]+z_M[M] + (z_M+1)[HM]+z_K[K]=0.$$

Considering small gradients, we linearize and combine the previous equations to keep only the three variables proton concentration $[H]$, total mobile buffer concentration c_M, and potential ψ:

$$\vec{J}_H^m+(1-\alpha)\vec{J}_{HM}^m-\alpha\vec{J}_M^m=-(D_h+\gamma_M D_M)(\nabla h+h\nabla\psi),$$

$$\vec{J}_M^{tot}=\vec{J}_M^m+\vec{J}_{HM}^m=-D_M(\nabla c_M+z'_M c_M\nabla\psi), \qquad \text{(B1)}$$

$$-z_K\frac{\vec{J}_K^m}{D_K}-z'_M\frac{\vec{J}_M^{tot}}{D_M}=-(1+\gamma_M+\gamma_F)\nabla[H] + (z'^2_M c_M+z_K^2[K])\nabla\psi$$

Where

$$\gamma_F=\frac{c_F K_F}{([H]+K_F)^2}, \quad \gamma_M=\frac{c_M K_M}{([H]+K_M)^2},$$

$$\alpha=\frac{[H]}{[H]+K_M}=\frac{[HM]}{[HM]+[M]}$$

is the non-dissociated acid fraction, and $z'_M=z_M+\alpha$ is the total charge of the mobile buffer [i.e., the one of $(1-\alpha)M+\alpha HM$].

[1] *Tip Growth in Plant and Fungal Cells*, edited by, I.B. Heath (Academic, San Diego, 1990).
[2] P. Pelcé, *Théorie des Formes de Croissance* (CNRS Editions, Paris, 1999).
[3] H.G.E. Hentschel and A. Fine, Phys. Rev. Lett. **73**, 3592 (1994); B. Denet, Phys. Rev. E **53**, 986 (1996); R. Kam and H. Levine, Phys. Rev. Lett. **79**, 4290 (1997).
[4] N.A.R. Gow, J. Gen. Microbiol. **130**, 3313 (1984).
[5] N.A.R. Gow, Microbiology **140**, 3193 (1994).
[6] C.L. Slayman and C.W. Slayman, Science **136**, 876 (1962).
[7] L.F. Jaffe and R. Nuccitelli, J. Cell Biol. **63**, 614 (1974).
[8] D.L. Kropf, J.H. Caldwell, N.A.R. Gow, and F.M. Harold, J. Cell Biol. **99**, 486 (1984).
[9] The relative effects of convection and diffusion are determined by the Peclet number $Pe\sim UL/D$ where $U\sim10^{-7}$m/s is the hyphal growth rate, $L\sim10^{-3}$m is the typical length and $D\sim10^{-9}$m^2/s the diffusion coefficient. Using these values, $Pe\sim0.1$ indicates that diffusion dominates.
[10] D.L. Kropf, J. Cell Biol. **102**, 1209 (1986).
[11] D.H. Jennings, in *Fungal Walls and Hyphal Growth*, edited by J.H. Burnett and A.P.J. Trinci (Cambridge University Press, Cambridge, 1979).
[12] P. Pelcé, Phys. Rev. Lett. **71**, 1107 (1993); M. Léonetti and E. Dubois-Violette, Phys. Rev. E **56**, 4521 (1997).
[13] T.V. Potapova, K.B. Aslanidi, T.A. Belozerskaya, and N.N. Levina, FEBS Lett. **241**, 173 (1988).
[14] K.B. Aslanidi, O.V. Aslanidi, D.M. Vachadze, O.A. Mornev, T.V. Potapova, L.M. Chailakhyan, and E.G. Shtemanetyan, Membr. Cell Biol. **11**, 349 (1997).
[15] L. Limozin, B. Denet, and P. Pelcé, Phys. Rev. Lett. **78**, 4881 (1997).
[16] S. Bartnicki-Garcia, F. Hergert, and G. Gierz, Protoplasma **154**, 46 (1989).
[17] Y. Saito, G. Goldbeck-Wood, and H. Muller-Krumbhaar, Phys. Rev. A **38**, 2148 (1988).
[18] D. Sanders, U.-P. Hansen, D. Gradmann, and C.L. Slayman, J. Membr. Biol. **77**, 123 (1984).
[19] J.J. Gits and M. Grenson, Biochim. Biophys. Acta **135**, 507 (1967).
[20] M.L. Pall, Biochim. Biophys. Acta **233**, 201 (1970).
[21] W.J.A. Schreurs, R.L. Harold, and F.M. Harold, J. Gen. Microbiol. **135**, 2519 (1989).
[22] F.M. Harold, Microbiol. Rev. **54**, 381 (1990).
[23] R. Larter and P. Ortoleva, J. Theor. Biol. **88**, 599 (1981).
[24] M. Léonetti, Eur. Phys. J. B **2**, 325 (1998).
[25] M. Léonetti and E. Dubois-Violette, Phys. Rev. Lett. **81**, 1977 (1998).
[26] L. Limozin, Ph.D. thesis, Aix-Marseille I, 1999.
[27] J. Ferrier, J. Theor. Biol. **85**, 739 (1980).
[28] L.F. Jaffe, K.R. Robinson, and R. Nuccitelli, Ann. N. Y. Acad. Sci. **9**, 372 (1974).
[29] D. Sanders, in *Solute Transport in Plant Cells and Tissues*, edited by D.A. Baker and J.L. Hall (Longman Scientific, New York, 1988).
[30] D. Sanders and C.L. Slayman, J. Gen. Physiol. **80**, 377 (1982).
[31] W.J.A. Schreurs and F.M. Harold, Proc. Natl. Acad. Sci. U.S.A. **85**, 1534 (1988).
[32] S.L. Jackson and I.B. Heath, Microbiol. Rev. **57**, 367 (1993).
[33] G.D. Robson, E. Prebble, A. Rickers, S. Hosking, D.W. Denning, A.P.J. Trinci, and W. Robertson, Fungal Genet. Biol. **20**, 289 (1996).

[34] C.L. Bachewich and I.B. Heath, Fungal Genet. Biol. **21**, 76 (1997).

[35] R.M. Parton, S. Fischer, R. Malho, O. Papasouliotis, T.C. Jelitto, T. Leonard, and N.D. Read, J. Cell. Sci. **110**, 1187 (1997).

[36] C.W. Cho, F.M. Harold, and W.J.A. Schreurs, Exp. Mycol. **15**, 34 (1991).

[37] H. Ammann, J. Noel, A. Tejedor, Y. Boulanger, A. Gougoux, and P. Vinay, Can. J. Physiol. Pharmacol. **73**, 421 (1995).